Mesoscopic magnetomechanical hysteresis in a magnetorheological elastomer

A. M. Biller,[1,*] O. V. Stolbov,[1,2,†] and Yu. L. Raikher[1,3,‡]

[1]*Institute of Continuous Media Mechanics, Russian Academy of Sciences, Ural Branch, Perm, 614013, Russia*

[2]*Perm National Research Polytechnic University, Perm, 614990, Russia*

[3]*Ural Federal University, Ekaterinburg, 620083, Russia*

(Received 25 March 2015; revised manuscript received 22 June 2015; published 26 August 2015)

Field-induced magnetostatic interaction in a pair of identical particles made of a magnetically soft ferromagnet is studied. It is shown that due to saturation of the ferromagnet magnetization, this case differs significantly from the (super)paramagnetic one. A numerical solution is given, discussed, and compared with that provided by a simpler model (nonlinear mutual dipoles). We show that for multidomain ferromagnetic particles embedded in an elastomer matrix, as for paramagnetic ones in the same environment, pair clusters may form or break by a hysteresis scenario. However, the magnetization saturation brings in important features to this effect. First, the bistability state and the hysteresis take place only in a limited region of the material parameters of the system. Second, along with the hysteresis jumps occurring under the sole influence of the field, the "latent" hysteresis is possible which realizes only if the action of the field is combined with some additional (nonmagnetic) external factor. The obtained conditions, when used to assess the possibility of clustering in real magnetorheological polymers, infer an important role of mesoscopic magnetomechanical hysteresis for the macroscopic properties of these composites.

DOI: 10.1103/PhysRevE.92.023202 PACS number(s): 41.20.Gz, 75.50.Tt, 81.05.Zx

I. INTRODUCTION

Magnetorheological (MR) polymers, magnetoactive elastomers, ferrogels, etc., all these terms designate polymer composites filled with ferromagnetic microparticles. If the initial (zero-strain) elastic modulus of such a material is sufficiently low (100 kPa range), the composite displays strong magnetomechanical effect under moderate ($\sim$1 kOe) fields. The phenomenon is yet more pronounced in case of a ferrogel where the matrix is made of a polymer gel or hydrogel, so that the effective modulus is just few tens of kPa.

In general, MR polymers and ferrogels altogether could be termed as materials with magnetic field-tuned rheology, which originates from intrinsic coupling between the components. This coupling is rather complicated since it emerges as a result of a number of interactions. First, under the influence of external field the particles, initially multidomain and thus demagnetized, acquire magnetic moments and via them enter in the long-range magnetostatic interaction with each other. The occurring distribution of anisotropic magnetic forces strives to organize the particles, e.g., in chains or strands. As the particles are sitting in a polymer matrix, their tendency to move in response to the field is opposed by the elastic (restoring) forces. Being induced by the particles, the elastic forces, which are also long range and anisotropic, are nonuniformly distributed over the sample. Therefore, the observed macroscopic behavior of a MR polymer reflects the net action of multiple processes establishing magnetoelastic balance at the mesoscopic (interparticle distance) scale. In technologically interesting MR systems, where the volume fraction of particles ranges in tens of percent, the particle size and the interparticle distances are of the same order of magnitude that sets the mesoscopic scale to units of microns.

The theory of MR composites in question is closely related to that of electrorheological (ER) and magnetorheological suspensions, and to a good extent borrows from the latter [1–3]. Certain essential differences should be remarked, however. First, in MR polymers the particles are not free to move in the matrix. Because of that, the aggregation processes governed in ER and MR suspensions solely by minimization of the electrostatic (magnetostatic) energy, in MR polymers never come "to the end" for they are counteracted by the matrix elasticity. Second is the difference between MR composites (either polymeric or fluid) and their ER analogs. Note that under any conceivable conditions the relation between the electric polarization and field may be taken as linear: $\boldsymbol{P} = (\varepsilon_p - \varepsilon)\boldsymbol{E}/4\pi$. This means that both dielectric permeabilities: ε_p, that of the particle substance (e.g., silica gel), and ε, that of the dispersing medium (matrix), do not depend on the field strength. Due to this constancy, the distribution of electric potential ψ in an ER system is determined by a Laplace equation ($\Delta\psi = 0$) with linear boundary conditions, so that the equation admits an exact solution whatever the number of the particles [4].

MR systems are different. As their microparticles are made of a ferromagnet, most typically of iron, in the absence of magnetic field, such particles are in the multidomain state, and their net magnetic moments are nearly zero. At relatively weak fields, the magnetization occurs mostly due to the growth of "favorable" domains, and in this regime it, albeit roughly, might be approximated by a linear law $\boldsymbol{M} = \chi_f^{(0)}\boldsymbol{H}$, where the initial internal susceptibility of a ferromagnet is rather high: $\chi_f^{(0)} \sim 10^3$–10^5 emu. With the increase of the field strength, the increase of M with H gradually slows down and finally attains saturation: $M \to M_s = \text{const}(H)$. One of the often used empirical relations accounting for nonlinear magnetization of multidomain iron samples is the Frölich-Kennelly formula [5–7], that incorporates both above-introduced

*Corresponding author: kam@icmm.ru

†oleg100@gmail.com

‡raikher@icmm.ru

material parameters:

$$M(H) = \frac{\chi_f^{(0)} M_s H}{M_s + \chi_f^{(0)} H} = \begin{cases} \chi_f^{(0)} H & \text{for} \quad \chi_f^{(0)} H \ll M_s, \\ M_s\left(1 - M_s/\chi_f^{(0)} H\right) & \text{for} \quad \chi_f^{(0)} H \gg M_s; \end{cases} \quad (1)$$

we note that hereafter the magnetization is assumed to be isotropic.

Apparently, the magnetization law (1) is equivalent to introducing the nonlinear susceptibility and permeability as

$$\chi_f(H) = \frac{\chi_f^{(0)} M_s}{M_s + \chi_f^{(0)} H}, \quad \mu_p(H) = 1 + 4\pi\chi_f(H). \quad (2)$$

In a nonconducting medium curl $\boldsymbol{H} = 0$, and this enables one to define the magnetostatic potential by the relation $\boldsymbol{H} = -\nabla\psi$ in full analogy with the electric case. However, under a nonlinear magnetization law, substitution of this equation in the solenoidal condition $\mathrm{div}(\boldsymbol{H} + 4\pi\boldsymbol{M}) = 0$ for the magnetic induction, instead of Laplace equation yields a nonlinear one

$$\Delta\psi = -\nabla\psi \cdot \nabla \ln \mu_p(-\nabla\psi), \quad (3)$$

the particular form of which is determined by the particular dependence of μ_p on the applied field. As well, nonlinear are the conditions imposed on the magnetostatic potential inside (i) and outside (e) of the physical boundary Γ of each particle:

$$\psi^{(i)}|_\Gamma = \psi^{(e)}|_\Gamma, \quad \mu_p(-\nabla\psi^{(i)}) \frac{\partial\psi^{(i)}}{\partial n}\bigg|_\Gamma = \mu \frac{\partial\psi^{(e)}}{\partial n}\bigg|_\Gamma, \quad (4)$$

where μ is the magnetic permeability of the polymeric matrix and $\boldsymbol{n}$ the outer normal to the surface. The nonlinearities imposed by Eqs. (3) and (4) are the essential feature of MR polymers. Due to that, the exact (linear) solutions of the Laplace equation, which suffice to deal with ER composites, are applicable to MR only when considering the range of initial magnetization ($\chi_f^{(0)} H \ll M_s$) where a ferromagnet responds in a quasiparamagnetic way.

In this paper, we consider and discuss the two-particle interaction problem with magnetic nonlinearities in the MR polymer context. For the systems in question, especially for those cured under zero field, it is a fundamental mesoscopic issue. Indeed, in such composites under zero field, the majority of the particles dwell as separated entities. The particle aggregation under the field is mechanically impeded by the polymer matrix, so that the number of emerging multiparticle chains is extremely low if any. On the other hand, taking into account the wide spread of interparticle distances in the ground state, it is natural to assume that the most probable field-induced structure patterns would be "dimer" aggregates. Given that, in the following we consider the field-induced behavior of a pair of particles positioned inside an elastic matrix at some distance from one another. Note that this problem statement differs essentially from that inherent to ER and MR suspensions. In the latter, the elastic resistance is absent, and the particles chain up without hindrance. Due to that, the fundamental mesoscopic issue for ER (MR) suspensions is the electrostatic (magnetostatic) force on a particle that sits tightly between others in a long one-dimensional aggregate (chain) and experiences the influence of a great many of neighbors from both sides. By now, this problem is studied to a detail analytically [8] as well as numerically [4,9–14].

II. MAGNETIC FIELD IN A SET OF TWO PARTICLES

Let two identical spherical particles of radius a be embedded in a nonmagnetic ($\mu = 1$) matrix with their centers positioned at a distance l. Vector $\boldsymbol{l}$ connects the particles 1 and 2 and makes the angle γ with the direction of the uniform external field $\boldsymbol{H}_0$. The coordinate framework for the problem is shown in Fig. 1, its center coincides with the center mass of the pair; axis Oz is directed along $\boldsymbol{H}_0$, while the plane yOz passes through vector $\boldsymbol{l}$. Taking a as a unit of length, we denote the intercenter distance as $q = l/a$, so that $q = 2$ corresponds to the close contact of the particles.

We assume that the particles are made of isotropic magnetically soft ferromagnet. The nonlinearity of the ferromagnet magnetization is described by the Frölich-Kennelly relation (1), the nondimensional strengths of the internal $\boldsymbol{H}$ and external $\boldsymbol{H}_0$ fields are introduced as

$$\boldsymbol{h} = \boldsymbol{H}/M_s, \quad \boldsymbol{h}_0 = \boldsymbol{H}_0/M_s. \quad (5)$$

In this representation, Eq. (1) takes the form

$$\boldsymbol{m} = \chi_f \boldsymbol{h}, \quad \chi_f = \frac{\chi_f^{(0)}}{1 + \chi_f^{(0)} h}, \quad (6)$$

with $\boldsymbol{m} = \boldsymbol{M}(\boldsymbol{H})/M_s$.

For the numerical solution of Eqs. (3) and (4), an iteration algorithm is used, which presents a nonlinear problem as a sequence of linear ones. The magnetostatic potential is evaluated inside a cube of finite size $d = \kappa(l + 2a)$, where $\kappa \gg 1$ is a numerical coefficient. Outside of the calculational region, ψ is defined as a sum of potentials of point dipoles, whose magnetic moments are equal to those of the considered particles evaluated at the preceding iteration step.

When the calculation begins, the susceptibility $\chi_f(\boldsymbol{r})$, which is nonzero only inside of the particles, is taken to be constant and equal $\chi_f^{(0)}$. Under this condition, the magnetostatic potential $\psi(\boldsymbol{r})$ is evaluated. By differentiating

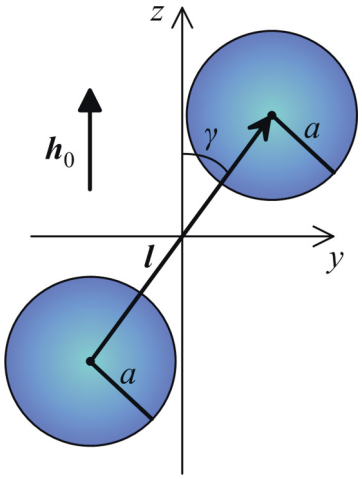

FIG. 1. (Color online) Coordinate frame for two-particle system.

it, one obtains the field $\boldsymbol{h}(\boldsymbol{r})$ in the entire space. From the spatial distribution of $\boldsymbol{h}$ inside the particles, a new set of values representing function $\chi_f(\boldsymbol{r})$ is constructed and used for the next step of the calculation. Therefore, at each iteration, a linear magnetostatic problem for a system with a spatially nonuniform susceptibility is solved, and this procedure is carried out until the magnetic moments of the particles stop to change.

The computer code implementing the above-mentioned algorithm is written in PYTHON language. It uses a finite-element method based at ESYS.ESCRIPT library. The calculational mesh is thickened in the regions where the largest gradients of the potential are expected. For that, the size λ_1 of the mesh elements residing on the particle surfaces, which face each other, is considerably diminished in comparison with λ_2, the size of an element on the "remote" parts of the particle surfaces. This is done under condition $\lambda_2 \ll \lambda_3$, where λ_3 is the mesh size near the outer boundary of calculational region. By varying the values of λ_{1-3} and κ, optimal balance between the accuracy of calculation and the amount of available computer resources is adjusted.

III. MAGNETIC INTERACTION FORCES

The magnetostatic problem (3) and (4) was solved for $\chi_f^{(0)} = 10^3$ in a wide range of the geometry parameters l and γ and the nondimensional field strength h_0. From this solution, the interaction energy of the pair is evaluated with the aid of formula

$$\frac{U_{\rm mag}}{M_s^2} = \int \left[\frac{1}{2}\boldsymbol{m}\cdot(\boldsymbol{h}-\boldsymbol{h}_0) - \int_0^h \boldsymbol{m}\cdot d\boldsymbol{h}\right] dV$$
$$= \int \left[\frac{1}{2}\boldsymbol{m}\cdot(\boldsymbol{h}-\boldsymbol{h}_0) - \frac{\chi_f^{(0)}|h| - \ln\left(\chi_f^{(0)}|h|+1\right)}{\chi_f^{(0)}}\right] dV, \tag{7}$$

obtained from the corresponding general relation [15]; integration in Eq. (7) is performed over the particle volumes. In result, a data array $U_{\rm mag}(h_0, l, \gamma)$ is obtained.

The magnetic interaction (ponderomotive) forces are rendered by the derivatives of the energy as

$$\boldsymbol{f} = \boldsymbol{f}_n + \boldsymbol{f}_\tau,$$
$$\boldsymbol{f}_n = -\frac{\boldsymbol{l}}{l^2}\left(\boldsymbol{l}\cdot\frac{\partial U_{\rm mag}}{\partial \boldsymbol{l}}\right), \quad \boldsymbol{f}_\tau = \frac{1}{l^2}\left[\boldsymbol{l}\times\left(\boldsymbol{l}\times\frac{\partial U_{\rm mag}}{\partial \boldsymbol{l}}\right)\right]. \tag{8}$$

As seen, vector $\boldsymbol{f}_n$ is directed along the center-to-center line $\boldsymbol{l}$ and determines the attraction (repulsion) force. Another component of the force $\boldsymbol{f}_\tau$ is perpendicular to $\boldsymbol{l}$ and lies in the plane made by vectors $\boldsymbol{h}_0$ and $\boldsymbol{l}$. The force couple $\boldsymbol{f}_\tau$ exerted on particles 1 and 2 induces the torque

$$\mathcal{M} = \boldsymbol{l}\times\boldsymbol{f}_\tau = -\boldsymbol{l}\times\partial U_{\rm mag}/\partial\boldsymbol{l}, \quad \mathcal{M} = -\partial U_{\rm mag}\partial\gamma$$

that strives to align the center-to-center line of the pair with the applied field.

The most simple and often used model of the particle magnetic interaction is the point dipole approximation. It is valid at $q = l/a \gg 1$ and certainly applies to the MR assemblies with homogeneous distribution and low concentration of the particles. In dense MR systems, the particles in majority are so close to one another that their intercenter distances are of the order of their own size: $q \gtrsim 2$. In this situation, the point dipole model fails since a substantial contribution to the interparticle forces comes from the nonuniform magnetization which the particles induce in one another. For the case of linear polarization ($\chi_f = \text{const}$), the problem could be solved rigorously for any q in terms of multipole expansion [4]. Quite expectedly, the differences between the predictions of linear models (the dipole and the multipole) increase when the interparticle distance is reduced ($q \to 2$); for the particles in contact this discrepancy ranges to orders of magnitude [11,16,17]. However, the common property of these solutions is the quadratic growth of the force: f_n, $f_\tau \propto h_0^2$ independently of the order of the multipole expansion. As remarked in the above, for real MR polymers the assumption of linear magnetization may be relied on only in weak field, and it necessarily breaks down at $h_0 \gtrsim 1$ where nonlinearity of the magnetization becomes relevant.

Saturation of magnetization entails saturation of the interparticle forces: they no longer depend on the applied field strength. This behavior is illustrated by Figs. 2 and 3 where those forces are plotted as functions of the field strength for several values of the interparticle distance l. In these graphs, solid lines show the results of our numerical calculation with allowance for the saturation effect while the parabolic curves correspond to the solutions based on the linear magnetization law with the number of multipoles about 100. The dashed lines are obtained with the aid of a simplified saturation

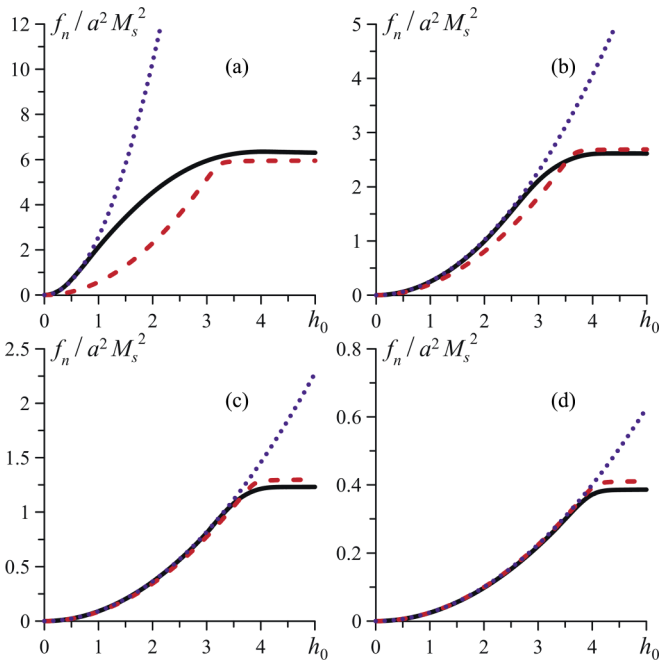

FIG. 2. (Color online) Attraction force for the head-to-tail configuration as a function of applied field for intercenter distances $q = 2.05$ (a), 2.5 (b), 3 (c), 4 (d); numerical solutions (solid lines), multipole expansion with linear magnetization (dots), NMD model (dashes). As the magnetic force rapidly falls down with the interparticle distance, vertical scales of the plots are different.

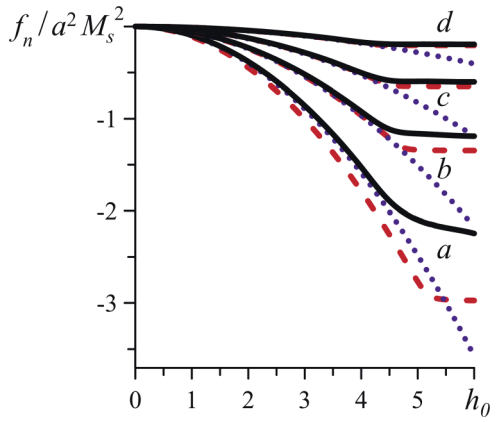

FIG. 3. (Color online) Repulsion force for the side-by-side configuration as a function of applied field for intercenter distances $q = 2.05$ (a), 2.5 (b), 3 (c), 4 (d); numerical solutions (solid lines), multipole expansion with linear magnetization (dots), NMD model (dashes).

model, where the particles are considered as point dipoles. The latter approximation, which we term *nonlinear mutual dipoles* (NMD), extends the linear dipole models introduced in [18,19]. A brief account of the NMD model is given in the Appendix.

As seen from Fig. 2, for the head-to-tail ($\gamma = 0^\circ$) configuration, the field of the neighbor contributes substantially to the particle saturation. For example, for $q = 2.05$ the linear multipole expansion [Fig. 2(a)] breaks down already at $h_0 \lesssim 1$. The same figure evidences that at small interparticle distances the NMD model, which accounts for nonlinearity but assumes uniformity of the particle magnetization, fails as well.

When the particles are not too close ($q \geqslant 3$), all the solutions resemble one another up to the crossover region, where the magnetization passes from increase to saturation. Under further growth of the field, the NMD model fairly well reproduces the numerical solution while the linear magnetization approximation hopelessly overestimates the interparticle force. For the repulsion forces ($\gamma = 90^\circ$), as Fig. 3 shows, the NMD model becomes reasonably valid already at $q \geqslant 2.5$.

Comparing Figs. 2 and 3, one finds that the interaction forces in the head-to-tail and side-by-side particle configurations saturate at different values of the magnetic field. For example, at $q = 2.5$ the attraction force attains maximum at $h_0 \sim 3.5$, although at the same value of q the repulsion force is yet about half-maximum. This difference has a simple explanation. In the head-to-tail configuration, the particle magnetization is enhanced due to the presence of its neighbor and by that brought closer to saturation. In the side-by-side pattern the presence of a neighbor reduces the field inside a given particle and, thus, diminishes its magnetization.

In Fig. 4, the dependence of the attraction and repulsion forces on the interparticle distance for the head-to-tail pattern is presented. As seen, with allowance for saturation, the applicability of a model depends on the field strength. If the field h_0 is far from the saturation range, the particle mutual approach augments the local field h and, thus, induces a considerable increase of magnetization. Due to that, in

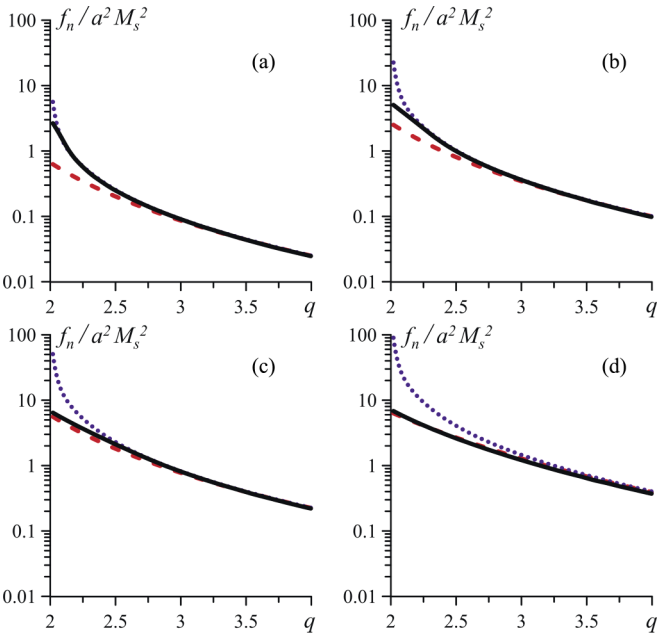

FIG. 4. (Color online) Attraction force for the head-to-tail configuration as a function of intercenter distance for the field strength $h_0 = 1$ (a), 2 (b), 3 (c), 4 (d); numerical solutions (solid lines), multipole expansion with linear magnetization (dots), NMD model (dashes).

Fig. 4(a) the exact solution looks very much like that for linearly polarizable particles (points). In a strong external field, which is capable by itself to bring the particles to saturation [the situation shown in Figs. 4(c) and 4(d)], the NMD model (dashes) fairly well reproduces the exact solution.

For the side-by-side pattern (see Fig. 5), the local field results in mutual demagnetization of the particles. Because of that, inside the particles even a seemingly strong external field is reduced to such extent that the transition to saturation is substantially "postponed." As a result, the model that assumes linear magnetization of the particles (points) is reasonably

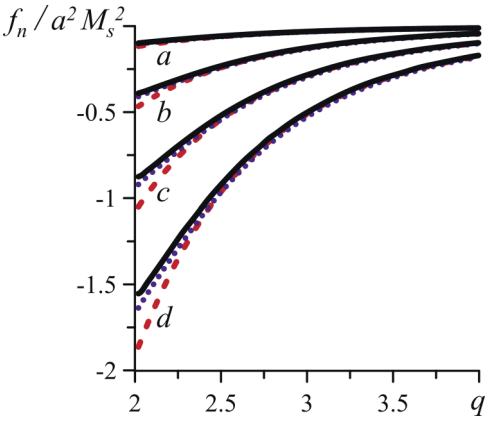

FIG. 5. (Color online) Repulsion force for the side-by-side configuration as a function of intercenter distance for the field strength $h_0 = 1$ (a), 2 (b), 3 (c), 4 (d); numerical solutions (solid lines), multipole expansion with linear magnetization (dots), NMD model (dashes).

close to the exact solution for any field within the studied interval.

IV. MAGNETOMECHANICAL HYSTERESIS OF THE PARTICLE PAIR

For a pair of magnetizable particles embedded in a polymer, the forces of their magnetic and elastic interaction are mutually dependent. The situation is as follows. The external field magnetizes each of the particles making them the sources of nonuniform (local) fields. Therefore, the equilibrium distribution of magnetization inside a given particle is established under joint influence of the external field $\boldsymbol{H}_0$ and the local field $\boldsymbol{H}_l(\boldsymbol{q})$ of the neighbor. Let at zero field the particles be positioned at a distance $\boldsymbol{q}_0 = \boldsymbol{l}/a$. Switching on of $\boldsymbol{H}_0$ induces the magnetostatic force $\boldsymbol{f}(\boldsymbol{q}_0)$ on each particle, and due to that the interparticle displacement $\Delta\boldsymbol{q}$ occurs. Upon that, the local field is changed to $\boldsymbol{H}_l(\boldsymbol{q}_0 - \Delta\boldsymbol{q})$, which, in turn, affects the magnetization distribution inside each particle and, finally, the interparticle force. As the above-presented solutions show, a full account for the forces between magnetically soft particles is especially important when the particles are close, i.e., the MR system is dense ($2 < q_0 < 4$).

At each stage of the field-induced displacement, the magnetic forces are counteracted by the resistance of the matrix. The elastic forces are the greater the larger $\Delta\boldsymbol{q}$. Note that at short interparticle distances ($2 < q_0 < 4$), even small absolute shifts of the matrix produce large strains. This means that, when describing the elastomer, one has to take into account the nonlinearity of its elastic properties. We do that with the aid of the Mooney-Rivlin model which is known [20] to fairly well render the deformational behavior of hyperelastic polymers (elastomers).

To deal with the mechanical behavior of the pair, in Ref. [17], having first numerically solved a reference problem, we proposed an approximation for function $U_{\rm el}(q,q_0)$ that yields the elastic energy increment of the particles which have been moved along their intercenter line from the initial separation q_0 to q. Our formula uses an auxiliary scheme comprising three nonlinearly elastic cylindrical rods, whose material is described by the Mooney-Rivlin potential

$$\widetilde{W}_k = W_k/c_1 = [I_1(\mathbf{C}_k) - 3] + \widetilde{c}_2[I_2(\mathbf{C}_k) - 3], \qquad (9)$$

with $k = 1, 2, 3$. Here, c_1 and $\widetilde{c}_2 = c_1/c_2$ are the parameters characterizing elastomer, and the invariants of the Cauchy-Green tensors $\mathbf{C}_k$ are expressed through the strains λ_k of the rods as

$$I_1(\mathbf{C}_k) = 2/\lambda_k + \lambda_k^2, \quad I_2(\mathbf{C}_k) = 1/\lambda_k^2 + 2\lambda_k.$$

In these notations, the approximate formula for the elastic energy takes the form

$$U_{\rm el}/c_1 = \pi \sum_{k=1}^{3} (2 - \delta_{k1}) \widetilde{W}_k \, r_k^2 \, l_{k,0}, \qquad (10)$$

where the radii r_k and lengths $l_{k,0}$ of the rods are adjustable parameters. The table of them evaluated under assumption $\widetilde{c}_2 = 0.1$ is given in Ref. [17]. There, it is shown that function (10) with good accuracy reproduces the numerical solution for intercenter distances $q_0 \geqslant 2.5$ and renders fairly reasonable results for smaller q_0, where the numerical calculation is unstable.

Evidently, our consideration treats the particles in a discrete (mesoscopic) way: as magnetic entities of finite size, while the matrix is described with the model taken from macroscopic rheology. There is no inconsistency, however. The reference scale we deal with is defined by the particle size, i.e., microns. In a soft elastomer, the size of structure elements (segments or blobs) ranges from units to tens of nanometers, i.e., is orders of magnitude lower. This means that at the micron scale the rheology of the matrix does not differ substantially from that displayed by it at the macroscopic (centimeter) scale, for which the here adopted model was originally proposed and is well justified [20].

Summing up the magnetic and elastic terms, i.e., Eqs. (7) and (10), one gets the energy of a pair of ferromagnet microparticles embedded in elastomer in the head-to-tail (with respect to the external field) configuration. This function is

$$U = U_{\rm mag}(h_0,q)|_{\gamma=0} + U_{\rm el}(q,q_0), \qquad (11)$$

where $U_{\rm mag}$ depends parametrically on $\chi_f^{(0)}$ and M_s [see formula (1)], and $U_{\rm el}$ on the Mooney-Rivlin constants c_1 and c_2.

Minimization of energy U with respect to q under given values of the external field h_0 and initial intercenter distance q_0 determines the equilibrium size of the pair. Analysis of function $U(h_0,q,q_0)$ reveals that in a certain applied field range, it has two coexisting minima. This means that the system displays magnetomechanical bistability. Namely, the enhancement of field up to certain value $h_0^{(1)}$ might induce a collapse of a pair in a tight cluster: $q \simeq 2$. This effect occurs in a hysteretic manner (the first-order transition): under diminution of the field the cluster breaks apart at the field $h_0^{(2)} < h_0^{(1)}$. We note that the considered particles are of micron size and, thus, are massive enough to entirely neglect the effect of Brownian motion on the transition thresholds.

To characterize the ability of the system for transitions, we rewrite Eq. (11) as

$$\widetilde{U}(h_0,q,q_0) = U/(c_1 a^3) = \beta \widetilde{U}_{\rm mag}(h_0,q) + \widetilde{U}_{\rm el}(q,q_0), \qquad (12)$$

thus introducing nondimensional energies $\widetilde{U}_{\rm mag} = U_{\rm mag}/(M_s a^3)$ and $\widetilde{U}_{\rm el} = U_{\rm el}/(c_1 a^3)$ convenient for calculations, and parameter

$$\beta = M_s^2/c_1, \qquad (13)$$

which defines the ratio of the energy of two magnetically saturated particles to their elastic energy in the matrix. In Fig. 6, the profiles of function $\widetilde{U}$ under varying field are shown. Depending on the value of β, two qualitatively different cases of bistability are encountered. The left panel shows the energy profile of the head-to-tail pair in a "soft" material ($\beta = 47$). As seen, in a weak field there exists only one energy minimum corresponding to an insignificant change of the initial size (curve 1). With the increase of the field, the second minimum emerges (curves 2 and 3): the system enters the bistability regime. Further on, the "far" minimum disappears (curve 4), and the only remaining stable state is the cluster one. Moreover, the position and depth of this only minimum cease to change

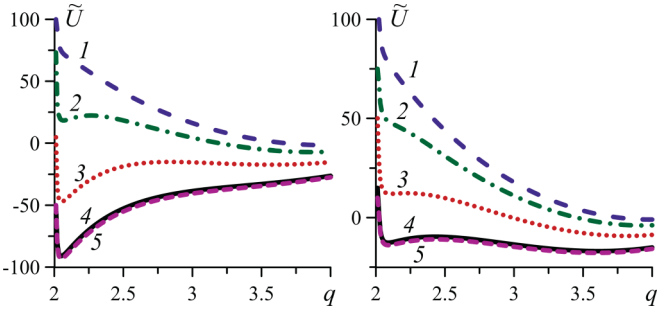

FIG. 6. (Color online) Interaction energy profiles at $q_0 = 4$ for "soft" ($\beta = 47$, left panel) and "rigid" ($\beta = 27$, right panel) systems under applied field $h_0 = 1$ (1), 2 (2), 3 (3), 4 (4), 5 (5).

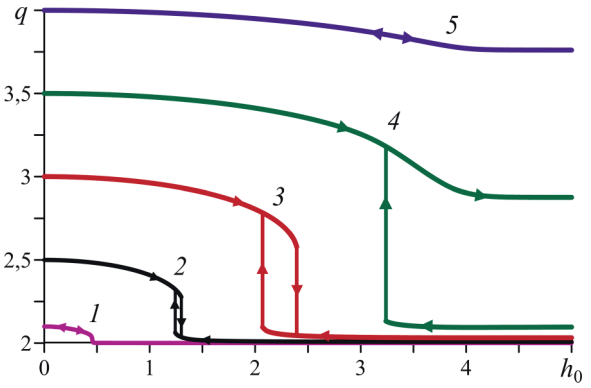

FIG. 7. (Color online) Interparticle distance as a function of the applied field strength for the pairs of different initial sizes: $q_0 = 2.1$ (1), 2.5 (2), 3 (3), 3.5 (4), 4 (5); parameter $\beta = 18$.

as soon as the particles become magnetically saturated (cf. curves 4 and 5).

In a more rigid system ($\beta = 27$) (see the right panel of Fig. 6), the bistability, having once occurred (curve 3), persists up to the values of the field strength which saturate the particle magnetization. As a result, the potential $\widetilde{U}$ retains its two-well profile however high h_0. In this case, the magnetomechanical hysteresis is "latent": the cluster state, although being possible, is never occupied since the "far" minimum never disappears. However, as seen from the right panel of Fig. 6, had a cluster formed somehow (in a strong field), then under the field diminution it would necessarily break up, and the particles would move apart to their initial intercenter distance q_0.

This bistability region is restricted with respect to the pair size. The upper bound $q_0^{(\mathrm{up})}$ is due to the nonlinearity of particle magnetization. Consider a perfect cluster whose intercenter distance is $q_* = 2$; under saturation, its magnetic energy attains absolute minimum $\widetilde{U}_* = \widetilde{U}_{\mathrm{mag}}(q_*)$, which value is finite and independent of h_0. Apparently, $-\widetilde{U}_*$ yields the maximum for magnetic energy decrement $\Delta\widetilde{U}_{\mathrm{mag}}$ under arbitrary change of interparticle distance. On the other hand, the increment of elastic energy equals $\Delta\widetilde{U}_{\mathrm{el}}(q_*,q_0)$, does not depend on the field, and grows unboundedly with q_0. This means that at q_0's large enough (e.g., in a dilute system) the elastic forces prevent clustering.

The lower bound $q_0^{(\mathrm{dn})}$ of the bistability region is imposed by the nonlinearity of the elastic force. Note that the Mooney-Rivlin model, like many others, reflects a fundamental fact that an elastomer becomes the stiffer the larger the strain. When the particles are very close ($q_0 \simeq 2$), then a small displacement entails large strain and, thus, high increment of the elastic energy. Thus, even upon driving closely positioned particles up to magnetic saturation, one is unable to notably change the interparticle distance: the medium in the gap becomes too stiff to be compressed by the magnetic forces available.

Therefore, one concludes that for the considered system, the bistability region is restricted to the range $(q_0^{(\mathrm{dn})}, q_0^{(\mathrm{up})})$. With the growth of saturation magnetization M_s of the ferromagnet and the softness of the matrix, this interval widens: the lower bound $q_0^{(\mathrm{dn})}$ decreases, while the upper bound $q_0^{(\mathrm{up})}$ grows.

Comparing the bistability properties of magnetically saturable (ferromagnetic) particles with those of linearly magnetizable (paramagnetic) ones studied in Ref. [17], we remark two essential differences. First, for paramagnetic particles the magnetic hysteresis could be induced at any pair size q_0 provided the field is strong enough. Second, an exclusive property of the saturating system is the lack of magnetomechanical hysteresis albeit the bistability is present.

Consider the state where under a certain value of h_0 the energy profile $\widetilde{U}(q)$ (due to the change of $\widetilde{U}_{\mathrm{mag}}$) has transformed from a single-well to a double-well one. If this occurs at h_0 that is close to the saturation level, then any further increase of the field does not affect $\widetilde{U}_{\mathrm{mag}}$, so that the energy function $\widetilde{U}$ becomes independent of h_0. In this case, the situation is bistable but the hysteresis remains "latent": the cluster state (the energy minimum at $q \simeq 2$) does exist but the system would not attain it whatever the field.

The afore given qualitative analysis makes it easy to understand the plots of Fig. 7 obtained with numeric calculations via Eq. (12), which present the field-induced deformations of the ferromagnet particle pairs of different initial size. As mentioned, for very close particles the alternative energy minima virtually coincide, and the cluster formation undergoes gradually (curve 1). The magnetomechanical hysteresis really emerges at larger initial sizes; for the assumed value $\beta = 18$ this interval is located at $2.5 < q_0 < 3.5$ (curves 2 and 3). There, the jumps of the intercenter distance are significant. At greater q_0, the hysteresis becomes "latent" (curve 4): under the increase or decrease of the field the actual deformation of the pair $q(h_0)$ remains single valued since only the upper branch of curve 4 works. Meanwhile, the bistability interval (the region where curve 4 is double valued) spans to infinity with respect to h_0. This implies that if a cluster is formed (due to some nonmagnetic intervention), the system would balance its intrinsic magnetic and elastic forces in such a way that this cluster would be stable under any field exceeding the threshold (curve 4, lower branch). For the pairs of yet larger size, the hysteresis is impossible (curve 5) because even under saturation the magnetic forces are too weak to match the elastic ones.

V. DISCUSSION AND CONCLUSIONS

Our results feature the field-induced mechanical response of ferromagnet particles embedded in an elastomer. Those particles have nonlinear (field-dependent) susceptibility, and

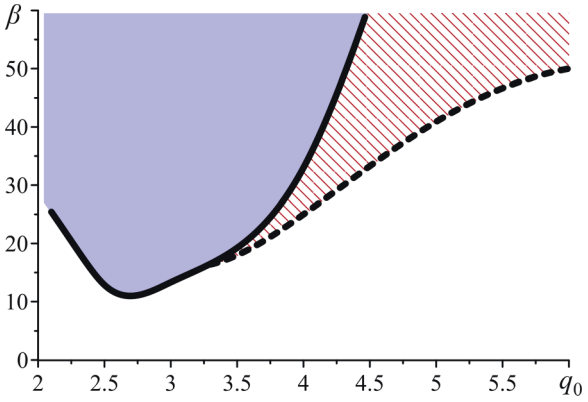

FIG. 8. (Color online) Diagram of states for magnetomechanical hysteresis in a pair of ferromagnet particles embedded in an elastic matrix and magnetized in head-to-tail configuration; the shaded region corresponds to realizable hysteresis, the hatched region to the "latent" one.

their magnetization cannot exceed the saturation level. Due to that, the interparticle forces depend on the field strength only within a certain range. By that, the ferromagnet case differs qualitatively from the paramagnet one, where the magnetic forces obey universal scaling $\propto H_0^2$, i.e., grow unboundedly. For a saturating ferromagnet, the forces do not scale as any fixed power of the field strength, that excludes constructing of handy approximations similar to those proposed for paramagnets in Refs. [17,19]. Quantitative difference with paramagnets is due to the fact that a ferromagnet (e.g., iron) has initial susceptibility $\chi_f^{(0)}$ that ranges 10^3–10^5 emu (see [5], for example), while for (super)paramagnets χ is orders of magnitude lower. For instance, according to Ref. [19], the susceptibility of the magnetic filling of Dynabead microspheres is $\sim 0.96/4\pi \simeq 0.08$ emu.

The magnetoelastic energy of a pair of magnetic particles embedded in an polymer is a combination of mutual attraction due to ponderomotive force and effective mutual repulsion caused by the elastic resistance of the matrix. As shown in Ref. [17], if the particles are paramagnetic, application of a field modifies this energy in such a way that the pair becomes bistable. In other words, there simultaneously exist two minima, one of which corresponds to an "expanded" pair (whose interparticle distance is close to the initial one), while another minimum favors a pair-cluster state. On the field growth beyond the bistability region, the first energy minimum disappears, and the cluster state remains the only one possible. Therefore, cluster formation in a paramagnetic pair evolves along the hysteresis scenario. Moreover, this effect occurs at any initial interparticle distance provided the field is strong enough.

The above-presented results predict that for ferromagnetic, i.e., magnetically saturating, particles the same scenario is possible as well. However, the saturation effect restricts occurrence of the magnetomechanical hysteresis to a limited parameter domain however strong is the field. Figure 8 presents the diagram of states for the considered "two-particle" MR polymer in the (q_0,β) plane. The solid line marks the border above which (shaded area) an abrupt transition to the cluster state could be induced solely by application of external field. The part in-between the solid and dashed lines (hatched area) corresponds to the bistability region, where hysteresis is "latent." By that we imply that the transition to cluster state might be provoked only by a combined action of the field and some other factor: mechanical stress, for example. We remark that the finite thickness of both lines in Fig. 8 reflects the accuracy of our calculations but, as seen, in the scale of the plot this uncertainty is not very significant.

The lowest point of the boundary in Fig. 8 has coordinates $q_0 \simeq 2.7$ and $\beta \simeq 11$. To the right of this point, the solid and dashed curves ascend, evidencing that the higher the saturation magnetization (at given elasticity of the matrix), the more remote particles are able to clusterize. In this connection we remark that for linearly magnetizable particles (no saturation) considered in Ref. [17], the value of M_s is formally infinity, so that $\beta = \infty$ as well. Because of that, in Fig. 8 the paramagnetic region is located infinitely upward, meaning that for paramagnetic particles the magnetomechanical hysteresis is possible for any initial intercenter size of the pair. The ascend of the boundary line $\beta(q_0)$ in Fig. 8 to the left of the minimum point is caused by the fact that the Mooney-Rivlin (as well as any other) elastomer stiffens under enhanced strain. In other words, to build up a cluster of the particles, which initially are positioned close to one another, requires enhanced magnetic force.

Evidently, the considered "two-particle" MR composite is far too simple a model to be justifiably applied to real materials. However, let us try it for estimating the parameters of an MR elastomer liable to mesoscopic hysteretic processes. The latter are believed to entail important macroscopic consequences, viz., drastic growth of the elastic modulus and the field-induced plasticity effect. To get to numerical values, we note that coefficients $c_{1,2}$ which define the magnitude of the Mooney-Rivlin potential (9) are related to the Young modulus E of the matrix as $E = 6c_1(1 + \widetilde{c}_2)$ [20]. At the minimum point of the diagram of Fig. 8, one has $\beta \sim M_s^2/c_1 \sim 10$ that upon substitution of $M_s^2 \sim 3 \times 10^6\,\mathrm{emu}^2$ (iron) sets the reference value to $E_* \sim 2 \times 10^6\ \mathrm{dyn/cm}^2 = 200$ kPa.

The obtained estimate E_*, being derived from the position of the lowest point of the border in Fig. 8, yields the maximal value of the modulus of a system allowing for magnetomechanical hysteresis. In typical soft MR elastomers, the Young modulus E_c obtained in macroscopic experiments ranges 20–100 kPa [21,22], i.e., is lower than E_*. Moreover, one should recall that the considered magnetomechanical hysteresis is a mesoscopic effect. Therefore, the value of E entering the estimates is the modulus of the polymer matrix itself and not the Young modulus of composite as a whole. To relate E and E_c, we assume a rubberlike elastomer filled with chemically inert solid spherical microparticles. At the particle volume fraction of about 25%–30%, the modulus E_c of such a system exceeds that of its matrix three to four times (see [23], for example). Setting $E_c = 3E$, from the reference range of E_c, one finds $E \sim$ 10–30 kPa, that fairly well ensures condition $E < E_* \sim 200$ kPa.

An external field, when applied to such an MR elastomer, should induce there abundant formation of clusters, twosome or multiparticle. Those aggregates fit very well the role of "magnetic staples" [24,25], which make and maintain the

intrinsic stress in the structure and live as long as the field is on. These entities are believed to cause the observed growth of elastic modulus and the transition of an MR material to plasticity state [21,26,27]. Another mechanism that contributes to the same is the "latent" hysteresis. As shown, this mode of clustering cannot develop in a sample that is entirely free from external stress. However, any mechanical test means imposing some deformations and, thus, stresses. These stresses may well transform a possible hysteresis to a real one, thus forming additional clusters, which, once having emerged, would exist until the field would turn too low. According to Fig. 8, with allowance for the latent hysteresis, the material parameter range within which clusters emerge widens considerably.

In conclusion, the two-particle model, notwithstanding obvious shortcomings of the latter, yields the estimates which are completely reasonable, at least by an order of magnitude. On this basis, we infer that mesoscopic magnetomechanical hysteresis, the origin of which is clarified here, is an important mechanism of structure rearrangement in MR elastomers. Evidently, in order to correctly account for it on the macroscopic level, the mesoscopic model should be "processed" with the aid of homogenization schemes developed, for example, in Refs. [28,29]. By that, the continuum equations of MR polymer magnetomechanics could be extended for the case of materials subjected to intense particle clusterization.

ACKNOWLEDGMENT

The work was supported by RFBR Grants No. 13-01-96056 and No. 14-02-96003 and Project No. MIG S26/617 from the Ministry of Education and Science of Perm Region.

APPENDIX: NONLINEAR MUTUAL DIPOLES MODEL

Nonlinear mutual dipoles (NMD) approximation assumes that the particles are so (i) small and (ii) so remote from one another ($a \ll l$), that the intrinsic magnetic field $\boldsymbol{H}$ always may be treated as uniform, and the same applies to the induced magnetization $\boldsymbol{M}$. The particle substance (a multidomain ferromagnet) magnetizes according to a certain nonlinear law and saturates in a strong field.

Consider a spherical particle of such a kind, whose magnetic susceptibility χ_f is isotropic. For this particle, the relation between the external field $\boldsymbol{H}_{\rm ext}$ and the internal one is given by the relation

$$\boldsymbol{H} = \boldsymbol{H}_{\rm ext} - \frac{1}{3}\chi_f \boldsymbol{H} = \boldsymbol{H}_{\rm ext} - \frac{\boldsymbol{\mu}}{3V}, \tag{A1}$$

where V is the particle volume. Possessing magnetic moment $\boldsymbol{\mu}$, the particle creates in the outer space the dipolar field

$$\boldsymbol{H}_d = -\frac{\boldsymbol{\mu}}{|r|^3} + 3\frac{(\boldsymbol{\mu}\cdot\boldsymbol{r})\boldsymbol{r}}{|r|^5}. \tag{A2}$$

Let there be a pair of such particles with the centers positioned at distance $\boldsymbol{l}$ from one another. Then, the field acting on the magnetic moment of particle 2 is a sum of the externally applied field $\boldsymbol{H}_0$ and the dipolar field of particle 1 that is given by formula (A2). Due to permutation symmetry $1 \leftrightarrow 2$, the magnetic moments of the particles as well as the respective dipolar fields are equal. Substituting the sum $\boldsymbol{H}_0 + \boldsymbol{H}_d$ in Eq. (13) and setting $\boldsymbol{r} = \boldsymbol{l}$, one gets the equation for evaluation of the magnetic moment of either particle:

$$\boldsymbol{\mu} = \chi\left[\boldsymbol{H}_0 - \frac{\boldsymbol{\mu}}{3V} - \frac{\boldsymbol{\mu}}{l^3} + 3\frac{(\boldsymbol{\mu}\boldsymbol{l})\boldsymbol{l}}{l^5}\right]. \tag{A3}$$

Consider for a pair of such particles the same situation as in Sec. IV, i.e., the head-to-tail configuration. In that case, all the fields are directed along $\boldsymbol{H}_0$, and in Eq. (A3) only one component is relevant. It yields

$$H = H_0 - \chi_f H\left(\frac{1}{3} - \frac{2V}{l^3}\right). \tag{A4}$$

We introduce nonlinear magnetization by substituting in Eq. (A4) the Frölich-Kennelly relation (6), and get as a result a quadratic equation for the nondimensional field $h = H/M_s$:

$$h^2 + \left(\frac{1}{\chi_f^{(0)}} - h_0 + \rho\right)h - \frac{h_0}{\chi_f^{(0)}} = 0, \quad \rho = \frac{1}{3} - \frac{2V}{l^3}. \tag{A5}$$

Upon substituting its solution in Eq. (6), we find the nondimensional magnetization m as a function of h_0, $\chi_f^{(0)}$, and ρ, that is in fact of l. Then, the particle magnetic moment is

$$\mu = mM_sV = \frac{\chi_f^{(0)} h M_s V}{1 + \chi_f^{(0)} h}, \tag{A6}$$

and from it the pair interaction energy $U_{\rm mag}^{\rm (dp)}$ is obtained. Differentiation of the latter renders the interparticle forces in the NMD approximation. Those results are shown in Figs. 2–5 by dashed lines.

[1] J. Stangroom, Electrorheological fluids, Phys. Technol. **14**, 290 (1983).
[2] P. M. Adriani and A. P. Gast, A microscopic model of electrorheology, Phys. Fluids **31**, 2757 (1988).
[3] T. E. Halsey, Electrorheological fluids, Science **258**, 761 (1992).
[4] H. J. H. Clercx and G. Bossis, Many-body electrostatic interactions in electrorheologocal fluids, Phys. Rev. E **48**, 2721 (1993).
[5] R. M. Bozorth, *Ferromagnetism* (Wiley, New York, 1993).
[6] C. H. Lee, F. Reitich, M. R. Jolly, T. Banks, and K. Ito, Piecewise linear model for field-responsive fluids, IEEE Trans. Magn. **37**, 558 (2001).
[7] G. Bossis, P. Khuzir, S. Lacis, and O. Volkova, Yield behavior of magnetorheological suspensions, J. Magn. Magn. Mater. **258-259**, 456 (2003).
[8] J. M. Ginder, L. C. Davis, and L. D. Elie, Rheology of magnetorheological fluids: Models and measurements, Int. J. Mod. Phys. B **10**, 3293 (1996).

[9] D. J. Klingenberg and C. F. Zukoski, Studies of the steady-shear behavior of electrorheological suspensions, Langmuir **6**, 15 (1990).

[10] J. M. Ginder and L. C. Davis, Shear stresses in magnetorheological fluids: Role of magnetic saturation, Appl. Phys. Lett. **65**, 3410 (1994).

[11] R. Tao, Q. Jiang, and H. K. Sim, Finite-element analysis of electrostatic interactions in electrorheological fluids, Phys. Rev. E **52**, 2727 (1995).

[12] L. C. Davis, Model of magnetorheological elastomers, J. Appl. Phys. **85**, 3348 (1999).

[13] G. Bossis, O. Volkova, S. Lacis, and A. Meunier, Magnetorheology: Fluids, structures and rheology, in *Ferrofluids*, Lecture Notes in Physics Vol. 594, edited by S. Odenbach (Springer, Berlin, Heidelberg, 2002), pp. 202–230.

[14] M. López-López, P. Kuzhir, and G. Bossis, Yield stress in magnetorheological suspensions near the limit of maximum-packing fraction, J. Rheology **56**, 1209 (2012).

[15] L. D. Landau, E. M. Lifshitz, and L. P. Pitaevskii, *Electrodynamics of Continuous Media* (Pergamon, New York, 1984).

[16] Y. Chen, A. F. Sprecher, and H. Conrad, Electrostatic particle-particle interactions in electrorheological fluids, J. Appl. Phys. **70**, 6796 (1991).

[17] A. M. Biller, O. V. Stolbov, and Yu. L. Raikher, Modeling of particle interactions in magnetorheological elastomers, J. Appl. Phys. **116**, 114904 (2014).

[18] E. E. Keaveny and M. R. Maxey, Modeling the magnetic interactions between paramagnetic beads in magnetorheological fluids, J. Comput. Phys. **227**, 9554 (2008).

[19] D. Du, F. Toffoletto, and S. L. Biswal, Numerical calculation of interaction forces between paramagnetic colloids in two-dimensional systems, Phys. Rev. E **89**, 043306 (2014).

[20] P. Oswald, *Rheophysics: The Deformation and Flow of Matter* (Cambridge University Press, Cambridge, UK, 2009).

[21] G. V. Stepanov, S. S. Abramchuk, D. A. Grishin, L. V. Nikitin, E. Y. Kramarenko, and A. R. Khokhlov, Effect of a homogeneous magnetic field on the viscoelastic behavior of magnetic elastomers, Polymer **48**, 488 (2007).

[22] X. L. Gong, L. Chen, and J. F. Li, Study of utilizable magnetorheological elastomers, Int. J. Mod. Phys. B **21**, 4875 (2007).

[23] J. S. Bergström and M. C. Boyce, Mechanical behavior of particle filled elastomers, Rubber Chem. Technol. **72**, 633 (1999).

[24] P. V. Melenev, V. V. Rusakov, and Yu. L. Raikher, Magnetic behavior of in-plane deformable dipole clusters, J. Magn. Magn. Mater. **300**, e187 (2006).

[25] P. V. Melenev, Yu. L. Raikher, G. V. Stepanov, V. V. Rusakov, and L. S. Polygalova, Modeling of the field-induced plasticity of soft magnetic elastomers, J. Intell. Mater. Syst. Struct. **22**, 531 (2011).

[26] L. V. Nikitin, G. V. Stepanov, L. S. Mironova, and A. I. Gorbunov, Magnetodeformational effect and effect of shape memory in magnetoelastics, J. Magn. Magn. Mater. **272–276**, 2072 (2004).

[27] S. S. Abramchuk, E. Yu. Kramarenko, G. V. Stepanov, L. V. Nikitin, G. Filipcei, A. R. Khokhlov, and M. Zrínyi, Novel highly elastic magnetic materials for dampers and seals: Part I. Preparation and characterization of the elastic materials, Polym. Adv. Technol. **18**, 883 (2007).

[28] P. Ponte Castañeda and E. Galipeau, Homogenization-based constitutive models for magnetorheological elastomers at finite strain, J. Mech. Phys. Solids **59**, 194 (2011).

[29] A. Menzel, Bridging from particle to macroscopic scales in uniaxial magnetic gels, J. Chem. Phys. **141**, 194907 (2014).